The SK channel blocker apamin inhibits slow afterhyperpolarization currents in rat gonadotropin-releasing hormone neurones

Masakatsu Kato, Nobuyuki Tanaka, Sumiko Usui and Yasuo Sakuma

Department of Physiology, Nippon Medical School, Tokyo 113-8602, Japan

Gonadotropin-releasing hormone (GnRH) neurones play an essential role in the hypothalamo-pituitary-gonadal axis. As for other neurones, the discharge pattern of action potentials is important for GnRH neurones to properly function. In the case of a luteinizing hormone (LH) surge, for example, GnRH neurones are likely to continuously fire for more than an hour. For this type of firing, GnRH neurones must have a certain intrinsic property. To address this issue, we investigated the voltage-gated Ca^{2+} currents and Ca^{2+}-activated voltage-independent K^+ currents underlying afterhyperpolarization, because they affect cell excitability. Dispersed GnRH neurones from adult GnRH-EGFP (enhanced green fluorescent protein) transgenic rats were cultured overnight and then used for an electrophysiological experiment involving the perforated patch-clamp configuration. The GnRH neurones showed five subtypes of voltage-gated Ca^{2+} currents, i.e. the T-, L-, N-, P/Q- and R-types. The GnRH neurones also showed a slow afterhyperpolarization current (I_{sAHP}), but not a medium one. It is reported that the SK channel blocker apamin (10 pM–100 nM) blocks a medium afterhyperpolarization current but not an I_{sAHP}. In contrast to previous reports, the I_{sAHP} observed in rat GnRH neurones was potently blocked by apamin. In addition, the GnRH neurones expressed transcripts for SK1–3 channels. The results indicate that rat GnRH neurones express all five subtypes of voltage-gated Ca^{2+} channels and exhibit an apamin-sensitive I_{sAHP}, which may allow continuous firing in response to a relatively strong depolarizing input.

(Resubmitted 22 March 2006; accepted 20 April 2006; first published online 20 April 2006)
Corresponding author M. Kato: Department of Physiology, Nippon Medical School, Sendagi 1, Bunkyo-ku, Tokyo 113-8602, Japan. Email: mkato@nms.ac.jp

Gonadotropin-releasing hormone (GnRH) neurones discharge action potentials to release GnRH from their nerve terminals in the median eminence, which controls the secretion of gonadotropin from the anterior pituitary. Therefore, we have to know how the excitability of GnRH neurones is determined to understand their functions. For example, a luteinizing hormone (LH) surge lasts a few hours. During this time, GnRH neurones are likely to persistently fire, which must be due in part to a certain intrinsic property of the neurones. Functional expression of a variety of ion channels is a key factor in membrane excitability (Hille, 2001). Here we focus on voltage-gated Ca^{2+} channels and K^+ channels, because these two families of channels are closely involved in cell excitability, and because their expression profile shows substantial diversity (for reviews, see Garcia *et al.* 1997; Jan & Jan, 1997; Catterall, 2000).

The expression profile of subtype-specific Ca^{2+} channels has been examined in GnRH neurones from neonatal and pubertal rats (Kato *et al.* 2003), from young and adult mice (Nunemaker *et al.* 2003), and in mouse clonal cell line GT1–7 (Watanabe *et al.* 2004). GnRH neurones from pubertal rats express all five subtypes of voltage-gated Ca^{2+} channels, whereas mouse GnRH neurones from young or adult animals lack T-type channels. Here we investigated the voltage-gated Ca^{2+} currents in GnRH neurones from adult rats to complete the study of the developmental changes in their expression profiles.

It is well established that afterhyperpolarization affects cell excitability (for a review, see Sah, 1996). Therefore, we studied the Ca^{2+}-activated K^+ current, which underlies afterhyperpolarization (AHP). Afterhyperpolarization is widely observed in the central nervous system, including the hypothalamus (for reviews, see Faber & Sah, 2003; Vogalis *et al.* 2003; Stocker, 2004). Channels for AHP have been cloned as SK1–3 (Kohler *et al.* 1996), and are blocked by the bee venom apamin (Romey *et al.* 1984; Blatz & Magleby, 1986). Afterhyperpolarization is classified as medium and slow AHP according to the decay time course

 DOI: 10.1113/jphysiol.2006.110155

(for a review, see Vogalis *et al.* 2003). The current for medium AHP (I_{mAHP}) decays with a time constant of 100–200 ms and is blocked by apamin, whereas the current for slow AHP (I_{sAHP}) is not affected by apamin, and the decay time constant ranges from several 100 ms to several seconds. It is believed that I_{mAHP} is carried through SK channels, because it is blocked by apamin (Zang & Krnjevic, 1987; Schwindt *et al.* 1988; Stocker *et al.* 1999; Sailer *et al.* 2002; Villalobos *et al.* 2004). The channel(s) for I_{sAHP}, however, have not been determined to date.

In this study, we investigated the expression profile of voltage-gated Ca^{2+} currents and I_{AHP} in rat GnRH neurones by means of perforated patch-clamp recording. We revealed the presence of all five subtypes of voltage-gated Ca^{2+} currents and of I_{sAHP} with high sensitivity to apamin.

Methods

Rats that express enhanced green fluorescent protein (EGFP) under the control of the GnRH promoter (Kato *et al.* 2003) were used in these studies. The rats had free access to water and rat chow, and were kept under a 14-h light, 10-h dark cycle. The oestrous cycle stage was monitored by means of vaginal smear histology. Rats aged 2–3 months were used. All experiments were performed with the approval of the Nippon Medical School Animal Care Committee.

Short-term dissociated culture

Brains were excised from rats under ether anaesthesia. The medial septum, diagonal band of Broca, organum vasculosum of the lamina terminalis (OVLT), and medial preoptic area were cut out with a razor and surgical blades. The sections were minced and treated with papain (21 U ml^{-1}; Funakoshi, Tokyo, Japan) for 40–60 min at 30°C with gentle agitation. The tissues were triturated with a 5 ml plastic pipette after several washes with MEM (Invitrogen, Grand Island, NY, USA). The cell suspension was subjected to discontinuous Percoll density gradient centrifugation composed of 1.0, 1.023, and 1.078 g ml^{-1} layers. The cells obtained from the middle layer were plated on polylysine-coated coverslips and then incubated overnight in Neurobasal-A medium (Invitrogen) supplemented with 0.5 mM L-glutamine, B-27 (Invitrogen), and 5 ng ml^{-1} basic FGF (Invitrogen) at 37°C. Most of the GnRH neurones were either round or spindle-shaped, and some of them possessed short processes.

Electrophysiology

A List EPC-9 patch-clamp system (HEKA Electronik, Lambrecht/Pfalz, Germany) was used for the recordings and data analyses. Whole-cell currents were measured by means of the perforated patch-clamp technique with amphotericin B (Seikagaku Corp., Tokyo, Japan; Kato *et al.* 2003) at room temperature (25°C). The final concentration of amphotericin B in the pipette solution was 0.05 mg ml^{-1}. The pipette solution consisted of (mM) 95 potassium aspartate, 47.5 KCl, 1.0 $MgCl_2$, 0.1 EGTA and 10 Hepes (pH 7.2), the osmolarity being adjusted to 270 mosmol l^{-1}. The extracellular solution consisted of (mM) 137.5 NaCl, 5 KCl, 2.5 $CaCl_2$, 0.8 $MgCl_2$, 0.6 $NaHCO_3$, 10 glucose and 20 Hepes (pH 7.4), the osmolarity being adjusted to 300 mosmol l^{-1}. To minimize non-specific binding of peptides, 0.01% cytochrome C (Wako Junyaku, Osaka, Japan) was included in the extracellular solution. For the recording of Ca^{2+} currents, K^+ was replaced by Cs^+ in the pipette solution, and KCl was replaced by CsCl and 10 mM NaCl was replaced by 10 mM tetraethylammonium chloride in the extracellular solution. In addition, 0.3 μM TTX (Seikagaku Corp., Tokyo, Japan) was included to block the Na^+ currents. Pipettes were fabricated from borosilicate glass capillaries and had a resistance of 6–8 MΩ. The pipettes were targeted to the GnRH neurones in the extracellular solution without cytochrome C. After the cell had been touched, slight negative pressure was applied to the pipette, which led to a seal resistance of ∼5 GΩ. Perforation with amphotericin B was achieved within 3–7 min after giga-seal formation. The currents were filtered at 2.3 kHz, digitized at 10 kHz and recorded. The series resistance was 70%, electronically compensated. Data were taken when the series resistance was stable and less than 30 MΩ. The leak currents ranged from −5 pA to −40 pA at −90 mV. The cell capacitance was 13.5 ± 3.3 pF ($n = 100$). Capacitative and leak currents were subtracted by means of the p/4 protocol. In current-clamp experiments, a few pico-amps were injected to keep the membrane potential around −70 mV when necessary. Action potentials were elicited with 2 s current pulses with 3 pA steps. The time of spike failure, instantaneous firing frequency and maximum hyperpolarization in the interspike interval were examined.

Single-cell RT-PCR

Coronal slices (200 μm thick) containing the medial septum, diagonal band of Broca, OVLT and medial preoptic area were prepared from adult female rats. The rats were decapitated under ether anaesthesia, and then their brains were quickly removed and immersed in an ice-cold oxygenated (95% O_2, 5% CO_2) cutting solution comprising (mM) 2.5 KCl, 1.25 Na_2HPO_4, 0.6 $NaHCO_3$, 0.5 $CaCl_2$, 7 $MgCl_2$, 10 Hepes, 7 glucose, 248 sucrose, 1.3 ascorbic acid and 3 Na pyruvate (pH 7.4, 290 mosmol l^{-1}). The brains were blocked, glued with cyanoacrylate to the chilled stage of a Vibratome VIB3000 (Vibratome,

St Louis, MO, USA), and cut. The slices were then incubated at 30°C for 30 min in oxygenated artificial cerebrospinal fluid (ACSF) containing (mM) 137.5 NaCl, 2.5 KCl, 1.25 Na_2HPO_4, 0.6 $NaHCO_3$, 2 $CaCl_2$, 2 $MgCl_2$, 10 Hepes and 10 glucose (pH 7.4, 290 mosmol l^{-1}), and thereafter kept at room temperature. Each slice was transferred to the recording chamber, held submerged, and continuously superfused with oxygenated ACSF at the rate of 3 ml min^{-1}. The slice was viewed under an upright fluorescence microscope (BX50; Olympus, Tokyo, Japan) with a 40× water-immersion objective lens. Pipettes of 2–3 MΩ were fabricated from glass capillaries baked at 200°C for 5 h. Each pipette was filled with 7.5 μl of an autoclaved solution comprising (mM) 150 KCl, 3 $MgCl_2$, 5 EGTA and 10 Hepes (pH 7.2, 270 mosmol l^{-1}). A small amount of positive pressure was applied to the pipette and then the pipette was targeted to GnRH neurones. After the cell had been touched, the positive pressure was removed, and negative pressure was applied for sealing and breaking of the patch membrane. The cytoplasmic contents were harvested under visual control and transferred to a thin-wall PCR tube containing 10 μl of a reaction mixture for reverse-transcription (Takara LA PCR Kit AMV version 3; Takara Bio, Shiga, Japan). The reaction mixture comprised 5 μM random 9mers and 8 U AMV reverse transcriptase XL (from Avian Myeloblastosis Virus), and the reaction conditions were 30°C (10 min), 50°C (30 min), 99°C (5 min), and 4°C (5 min). The RT reaction product from a single cell was used for the PCR reaction with Takara ExTaq (Takara Bio) according to the manufacturer's instructions. The PCR conditions were 95°C for 5 min, 45 cycles of 94°C for 30 s, 55°C for 30 s, and 72°C for 60 s, and finally 72°C for 5 min. The reaction products were separated on a 1.5% agarose gel and photographed. A 100 bp DNA ladder was used as a marker. The results were confirmed in three independent experiments. The following primers were used: rat SK1, 5′-ACGCATCCAGTCGCAGCA-3′ (GenBank accession no U69885; location, nt 515–nt 533) and 5′-GCCTTGGTGAGTTCCAACT-3′ (nt 875–nt 857); rat SK2, 5′-GCGAATACTCTAGTGGATCT-3′ (U69882; nt 2707–nt 2726) and 5′-TAGCTACTCTCAGATGAAGTT-3′ (nt 3020–nt 3000); and rat SK3, 5′-AAGATTGACCA-CGCCAAAGT-3′ (U69884; nt 2066–nt 2085) and 5′-CA-ACTGCTTGAACTTGTGTAT-3′ (nt 2487–nt 2467).

Chemicals

Nifedipine was obtained from Wako Junyaku. ω-Conotoxin GVIA(GVIA), ω-agatoxin IVA (Aga-IVA), SNX-482 and apamin were purchased from the Peptide Institute (Osaka, Japan).

Statistics

Data are expressed as means ± standard deviation (S.D.) unless otherwise stated. The Kruskal–Wallis test, paired or unpaired *t* test, and Peason's correlation coefficient test were used for statistical analysis. The significance level was set at $P < 0.05$.

Results

Voltage-gated Ca^{2+} currents

The cell was held at −90 mV and the membrane potential was stepped to various voltages (−60 mV to +60 mV in 10 mV increments) for 100 ms at 0.2 Hz to activate Ca^{2+} currents. Maximum amplitudes of -57 ± 26 pA pF^{-1} ($n = 33$) in females and -55 ± 20 pA pF^{-1} ($n = 11$) in males were observed at 0–10 mV. Only the current traces at +10 mV are shown in Fig. 1*A* for clarity. To examine the voltage-gated Ca^{2+} channel subtypes in rat GnRH neurones, pharmacological dissection was carried out with specific blockers. After the control current had been recorded, 10 μM nifedipine, 1 μM GVIA, 200 nM Aga-IVA, 100 nM SNX-482 and 50 μM Ni^{2+} were successively applied. SNX-482 (R-type channel blocker; Newcomb *et al.* 1998; Tottene *et al.* 2000) attenuated the initial peak currents by approximately 30%, and the L-type channel blocker nifedipine (Boll & Lux, 1985) reduced the currents by 18–27%. The N-type channel blocker GVIA (Tsien *et al.* 1988; Aosaki & Kasai, 1989) inhibited the currents by ∼20%. Aga-IVA (P/Q-type channel blocker; Randall & Tsien, 1995) and a low concentration of Ni^{2+} (50 μM; T-type channel blocker; Tottene *et al.* 2000) reduced the currents by ∼12% and 9.3%, respectively. There was no statistically significant difference in the expression profile of Ca^{2+} currents according to sex or oestrous cycle stage (Fig. 1*B*).

Afterhyperpolarization current (I_{AHP})

Most of the GnRH neurones showed I_{AHP}, which was elicited by a voltage protocol comprising a 100 ms voltage pulse to +30 mV, followed by a 5 s voltage-step to −50 mV (Fig. 2*A*). The holding potential was −90 mV and the voltage pulse was applied every 30 s. Example traces of I_{AHP} are shown in Fig. 2*B*. The total charge of I_{AHP} was measured between 5 ms after the offset of a voltage pulse to +30 mV, and the time when the current returned to the base line. The charge was divided by the cell capacitance to obtain the charge density, which ranged from 0.91 to 30.5 pC pF^{-1} in 60 GnRH neurones from adult rats. The value was 7.44 ± 8.18 pC pF^{-1}. The decay time constant was determined by exponential fitting, as shown in Fig. 2*A*. The value was 533.4 ± 334.5 ms, ranging between 179 ms and 1600 ms.

Simultaneous application of 100 μM Ni^{2+} and 200 μM Cd^{2+}, which completely blocks the voltage-gated Ca^{2+} currents, inhibited I_{AHP} by 74–84% (Fig. 3). The remaining current was subtracted from the control current to isolate the Ni^{2+}- and Cd^{2+}-sensitive current (Fig. 3*A* and *B*).

The SK channel blocker apamin (10 pM–100 nM; Romey *et al.* 1984) suppressed I_{AHP}. Apamin at a concentration of 10 pM inhibited I_{AHP} by $11.4 \pm 12.8\%$ ($n = 5$), and 0.1 nM apamin further suppressed I_{AHP} by $57 \pm 8\%$ ($n = 5$). Example traces with 0.1 nM and 100 nM apamin, and the subtracted currents are shown in Fig. 4*A* and *B*. Apamin (100 nM) inhibited I_{AHP} by 63–77% in 5–14 neurones from females at each oestrous cycle stage and from males (Fig. 3*C*). The charge of the subtracted current was measured, as shown in Fig. 2*A*. The charge density ranged from 0.72 pC pF^{-1} to 27.4 pC pF^{-1} in 100 nM apamin-sensitive current, and

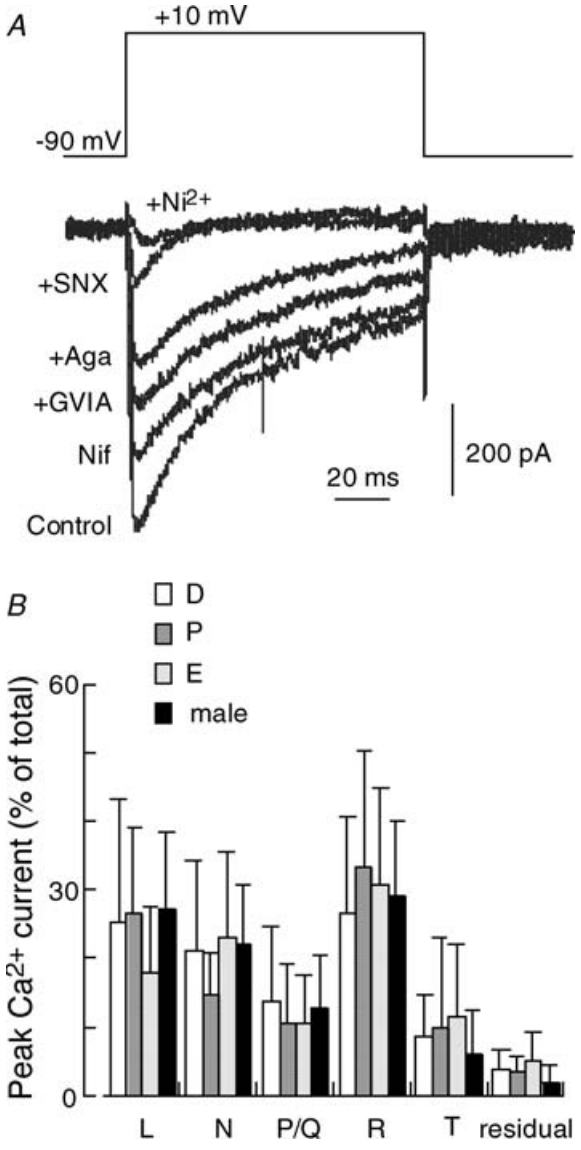

Figure 1. Voltage-gated Ca^{2+} currents in GnRH neurones
A, cells were held at −90 mV and given 100 ms voltage pulses (−60 to + 60 mV in 10 mV increments at 0.2 Hz). The voltage protocol and current traces activated by voltage pulse to +10 mV are shown. The current was attenuated by 10 μM nifedipine (Nif), 1 μM GVIA, 200 nM Aga-IVA (Aga), 100 nM SNX-482 and 50 μM Ni^{2+}. *B*, the effects of blockers are collectively shown as percentages of the total current ($n = 9$–13). The data show means ± S.D. The L-type current is the current blocked by nifedipine. The N-type, P/Q-type, R-type and T-type currents are those blocked by GVIA, Aga-IVA, SNX-482 and a low concentration of Ni^{2+}, respectively. Residual indicates the current resistant to all these blockers. The effects of blockers were statistically significant ($P < 0.01$, $n = 9$–13) in paired *t* test. There was no statistically significant difference according to either sex or oestrous cycle stage. D, di-oestrous; P, pro-oestrous; E, oestrous

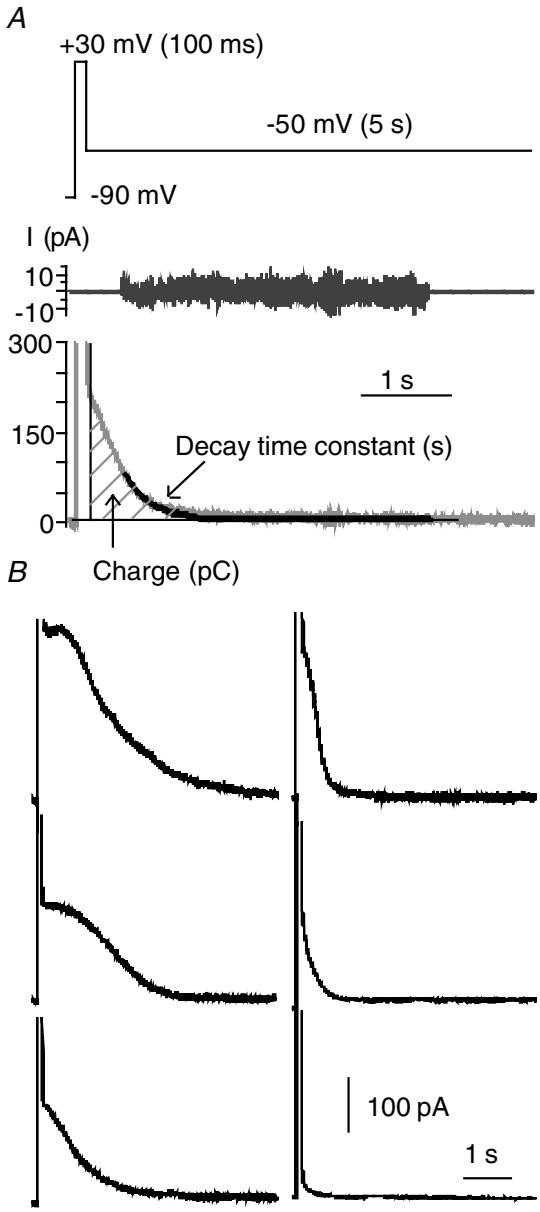

Figure 2. I_{AHP} in GnRH neurones
A, voltage-protocol and example trace. The holding potential was −90 mV, and 100 ms voltage-pulse to +30 mV followed by a 5 s voltage-step to −50 mV was delivered every 30 s. The total charge of I_{AHP} was measured between 5 ms after the offset of the voltage pulse to +30 mV and the time when the current returned to the baseline. The decay time constant of I_{AHP} was determined by exponential fitting, as shown in *A*. Residuals on exponential fitting are shown above the AHP current trace. The residuals were random, indicating a good fitting. *B*, representative examples of I_{AHP} observed in GnRH neurones. The traces shown are the averages of 5–10 traces.

from 1.16 pC pF^{-1} to 30.3 pC pF^{-1} in Ni^{2+}, Cd^{2+}-sensitive current (Fig. 3*D*). The median was 2.85–4.18 pC pF^{-1} in the apamin-sensitive current, and 3.25–5.92 pC pF^{-1} in the Ni^{2+}, Cd^{2+}-sensitive current. There was no statistically significant difference with regard to sex or oestrous cycle stage.

The decay time constant of both currents was determined by exponential fitting with IGOR Pro software (WaveMetrics, Lake Oswego, Oregon, USA), as shown in Figs. 2*A* and 4*A*. The subtracted traces clearly showed the presence of I_{sAHP} but not I_{mAHP}. The decay time constants ranged from 140 ms to 765 ms with a median of 285–321 ms in the apamin-sensitive currents, and from 153 ms to 799 ms with a median of 286–326 ms in the Ni^{2+}, Cd^{2+}-sensitive currents (Fig. 4*B*). There was no statistically significant difference according to sex or oestrous cycle stage. No clear concentration–response relationship was detected in the decay time constant of apamin-sensitive currents (data not shown).

A similar I_{AHP} was observed in six GnRH neurones examined in the acute slice preparation (Supplemental Fig. 1 online). The total charge of I_{AHP} was 95.2 ± 96.9 pC, ranging from 38 pC to 337 pC, and the decay time constant was 748 ± 454 ms, ranging between 275 ms and 1600 ms.

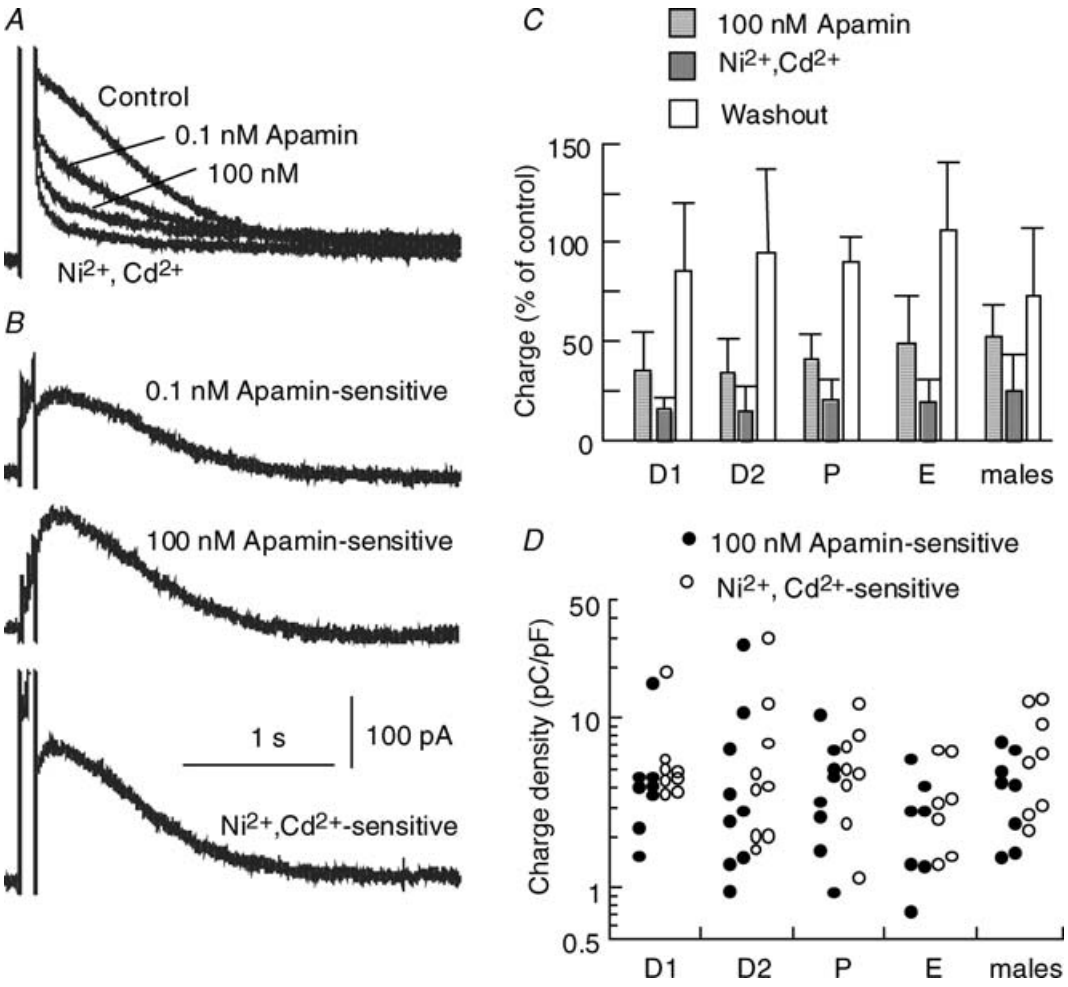

Figure 3. Effects of Ni^{2+} and Cd^{2+}, and apamin
A, example current traces. The voltage protocol was the same as in Fig. 2*A*. A concentration of 0.01–100 nM apamin attenuated the current, and the simultaneous application of 100 μM Ni^{2+} and 200 μM Cd^{2+} almost completely abolished the tail current. Current traces in the presence of 0.1 nM and 100 nM apamin are shown. *B*, the subtracted currents are shown, as apamin-sensitive and Ni^{2+}, Cd^{2+}-sensitive currents. *C*, collective presentation of the effects of blockers and washout. The data show means ± S.D. The effects of all the blockers were statistically significant at $P < 0.01$ ($n = 5$–14) in paired *t* test. *D*, charge densities (pC pF^{-1}) of individual apamin-sensitive (●) and Ni^{2+}, Cd^{2+}-sensitive (○) currents are plotted according to sex and oestrous cycle stage. There were no statistically significant differences among these groups in Kruskal–Wallis test. The *H*-values were 2.7 for apamin-sensitive current and 3.25 for Ni^{2+}, Cd^{2+}-sensitive current.

Effects of Ca^{2+} channel blockers on I_{sAHP}

As shown in Fig. 1, both low-voltage- and high-voltage-activated Ca^{2+} currents were observed in the GnRH neurones from adult rats. After the control I_{AHP} had been recorded, 10 μM nifedipine, 1 μM GVIA, 200 nM Aga-IVA, 100 nM SNX-482 and 50 μM Ni^{2+} were successively applied (Fig. 5). Some current traces are not shown in Fig. 5*A* for clarity. The data are from female neurones. In this experiment, data are not according to the oestrous cycle stage, because the oestrous cycle affected neither the Ca^{2+} currents nor I_{AHP}. Nifedipine attenuated the currents by $29.2 \pm 17.5\%$ and SNX-482 reduced them by $34.9 \pm 12.7\%$ in the 11 neurones examined. The

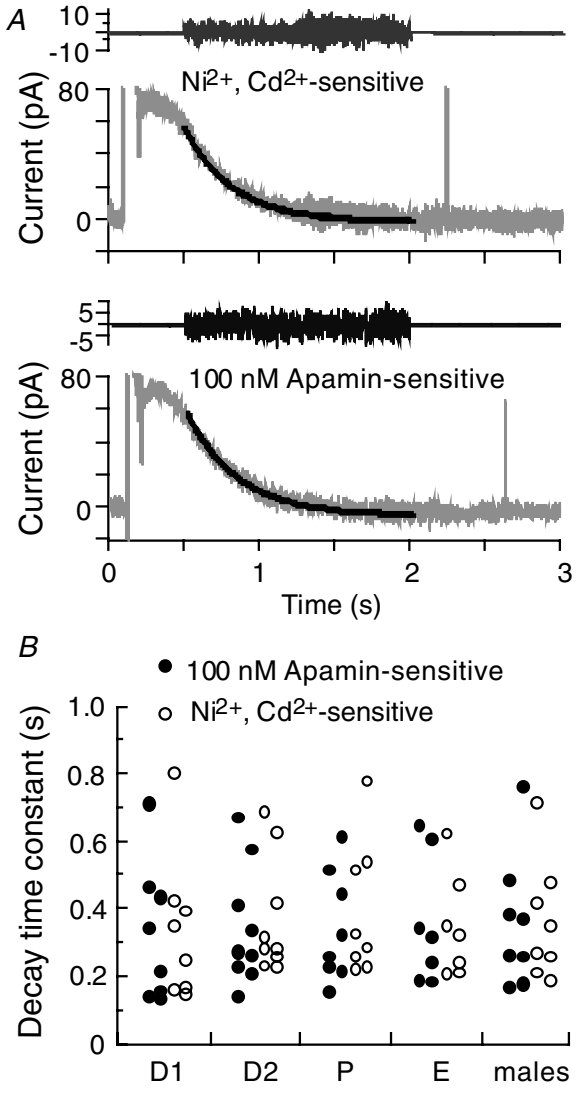

Figure 4. Decay time constant of I_{sAHP}
A, example traces of Ni^{2+}, Cd^{2+}-sensitive and apamin-sensitive currents recorded from the same cell. The decay time constants were 320 ms in the Ni^{2+}, Cd^{2+}-sensitive current and 340 ms in the apamin-sensitive current in this cell. The residuals on exponential fitting are shown above each current trace. *B*, decay time constant (s) of individual apamin-sensitive (●) and Ni^{2+}, Cd^{2+}-sensitive (○) currents are plotted according to sex and oestrous cycle stage. There were no statistically significant differences among these groups with the Kruscal–Wallis test. The *H*-values were 0.53 for apamin-sensitive current and 0.92 for Ni^{2+}, Cd^{2+}-sensitive current.

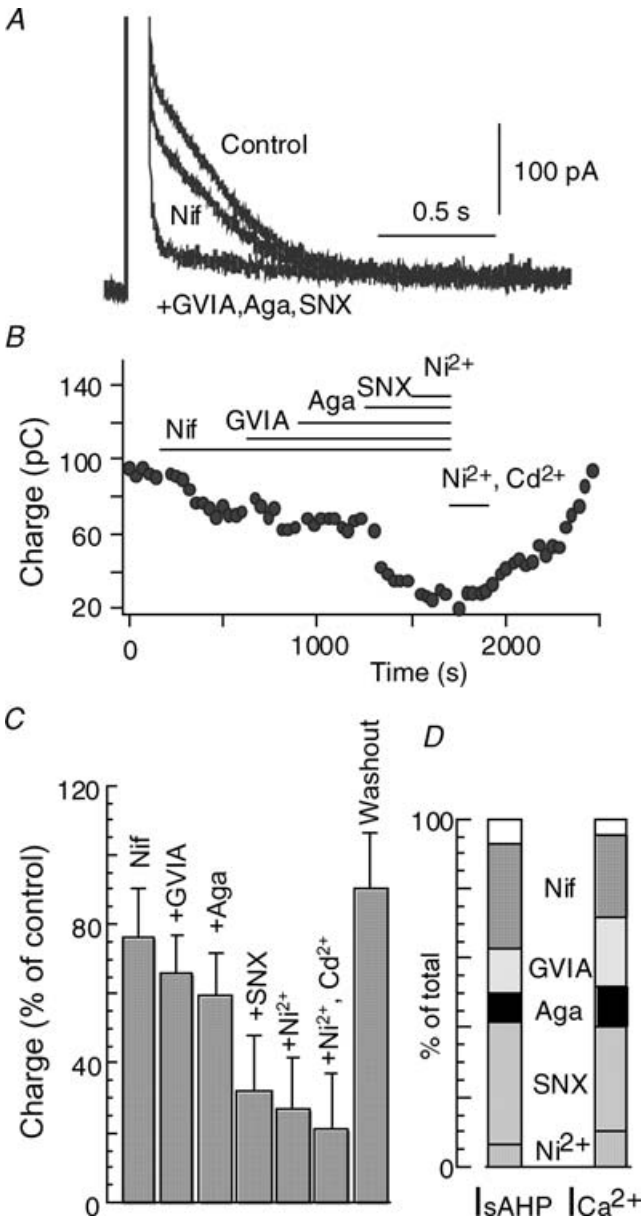

Figure 5. Effects of Ca^{2+} channel blockers on I_{AHP}
A, example traces recorded from female GnRH neurone are shown. The voltage protocol was the same as in Fig. 2*A*. Attenuations by nifedipine and the addition of GVIA, Aga-IVA and SNX-482 are shown. *B*, time course of the effects of blockers on the total charge of I_{AHP}. Blockers were applied as indicated by horizontal bars. *C*, the effects of blockers are collectively shown as percentages of the control. The data are from female neurones. The oestrous cycle stage was not determined in this experiment. The effect of each blocker was statistically significant at $P < 0.01$ ($n = 7$–11) in paired *t* test. *D*, combined presentation of the effects of Ca^{2+} channel blockers on both the Ca^{2+} current and I_{AHP}. The same data presented as those in Figs 1*B* and 5*C* were used. The percentage of Ni^{2+}, Cd^{2+}-sensitive component is shown for I_{sAHP}. The percentage blockade by each Ca^{2+} channel blocker was similar for the Ca^{2+} current and I_{sAHP}.

inhibitions by GVIA, Aga-IVA and Ni^{2+} were $13.3 \pm 7.7\%$, $8.2 \pm 5.2\%$ and $6.8 \pm 5.4\%$, respectively (Fig. 5*C*). The proportions of these currents are shown as percentages of the Ni^{2+}, Cd^{2+}-sensitive current together with Ca^{2+} currents (Fig. 5*D*). On average, the contribution of L-type Ca^{2+} current was 23.4% for the total Ca^{2+} current, and 30% for the activation of Ni^{2+}, Cd^{2+}-sensitive AHP current. The R-type current contributed 30.4% of the total Ca^{2+} current, and 35.5% of the Ni^{2+}, Cd^{2+}-sensitive AHP current.

Current-clamp experiments

Trains of action potentials were generated by 2 s current pulse with 3 pA increments (Fig. 6). At a low current intensity, GnRH neurones did not continue to discharge action potentials during a 2 s current pulse. This is a phenomenon known as spike frequency adaptation. When the current intensity increased, GnRH neurones fired action potentials to the end of the 2 s current pulse. At higher current intensity, however, the amplitude of action potentials progressively decreased during 2 s current pulse, and the cell finally failed to fire (see supplemental Fig. 2 online). When the amplitude of the action potential became less than 10% of that in the initial spike, it was defined as spike failure. The time of the last spike after the onset of the current pulse was taken as the time of spike failure (arrowheads in Fig. 6*B*). Under control conditions, spike failure started to occur in some neurones with a 12 pA current pulse and occurred in four out of the five neurones examined with a 30 pA pulse. Apamin accelerated the spike failure (Fig. 6*B* and *C*). Spike failure began in two out of the ten neurones examined with a 6 pA current pulse, and occurred in all five neurones examined with a 30 pA pulse in the presence of apamin. Spike failure was further accelerated by simultaneous application of Ni^{2+} and Cd^{2+}. The effects of these blockers were almost completely abolished on washout.

To characterize the spike frequency adaptation and spike failure, the instantaneous frequency and peak potential (maximum hyperpolarization) in the interspike interval were analysed. Figure 7*A* shows the initial five action potentials evoked by 27 pA current pulses in the control (upper trace) and in the presence of 100 nM apamin (lower trace). Under control conditions, the interspike interval (shown as instantaneous frequency in Fig. 7*B*) became broader in comparison to the first interval, and the amplitude of action potentials slightly decreased in the train of action potentials. In the presence of apamin, however, the broadening of the interspike interval was much less, and the reduction in amplitude of action potentials was greater (Fig. 7*A* and *B*). Apamin did not affect the first interval, but did shorten the second, third and fourth ones in comparison with the controls. Apamin also depolarized the membrane potential of the interspike interval. The peak potential in the interspike interval was slightly depolarized during the train of action potentials under control conditions, but apamin facilitated this depolarization, as shown in Fig. 7*A* (arrowheads). The effect of apamin was not observed in the first interspike interval, but was seen in the second interspike interval and through to the fourth one with a 12 pA current pulse, and the fifth one with an 18 pA pulse (Fig. 7*C*).

In 11 neurones examined in the current-clamp experiments, the charge density was 5.4 ± 3.4 pC pF^{-1}, ranging from 1.1 pC pF^{-1} to 11 pC pF^{-1}, and the decay time constant was 639 ± 147 ms, ranging from 496 ms to 988 ms under the control conditions. These values showed no correlation to the values of the time of spike failure, the instantaneous frequency and the peak potential of the interspike interval in Pearson's correlation coefficient test.

Transcripts for rat SK channels in GnRH neurones

To examine the expression of the SK channel mRNA in single GnRH neurones, RT-PCR analysis was performed (Fig. 8). RT-PCR with specific primers for SK1–3 yielded amplified products of the predicted size. A positive band for SK1 appeared in 5 of the 12 cells examined. One for SK2 was seen in 16 of the 19 cells examined and one for SK3 was seen in 15 of the 19 cells examined.

Discussion

The results show the presence of voltage-gated Ca^{2+} currents and a Ca^{2+}-activated voltage-independent slow afterhyperpolarization current (I_{sAHP}) in rat GnRH neurones. Neither current was affected by either the sex or oestrous cycle stage (Figs 1 and 3). All five subtypes of Ca^{2+} currents were seen in the adult GnRH neurones. The T-type Ca^{2+} current, however, is absent in neonates, becoming detectable around puberty (Kato *et al.* 2003). Another point is the high expression of the R-type current in neonates. The R-type current contributes ~60% of the total Ca^{2+} current in neonates and 40% around puberty. The expression profile of the subtype-specific Ca^{2+} currents in adult GnRH neurones (Fig. 1) is similar to that in pubertal GnRH neurones. So the T-type and R-type Ca^{2+} currents are developmentally regulated, and the adult expression profile is completed around puberty. The mouse GnRH neurone, however, lacks the T-type current and shows a low occurrence (15% of the total) of the R-type current (Nunemaker *et al.* 2003). In a clonal cell line of mouse GnRH neurones (GT1–7), 75% of the total Ca^{2+} current is carried through the R-type channel and no detectable current passes through the P/Q-type channel (Watanabe *et al.* 2004).

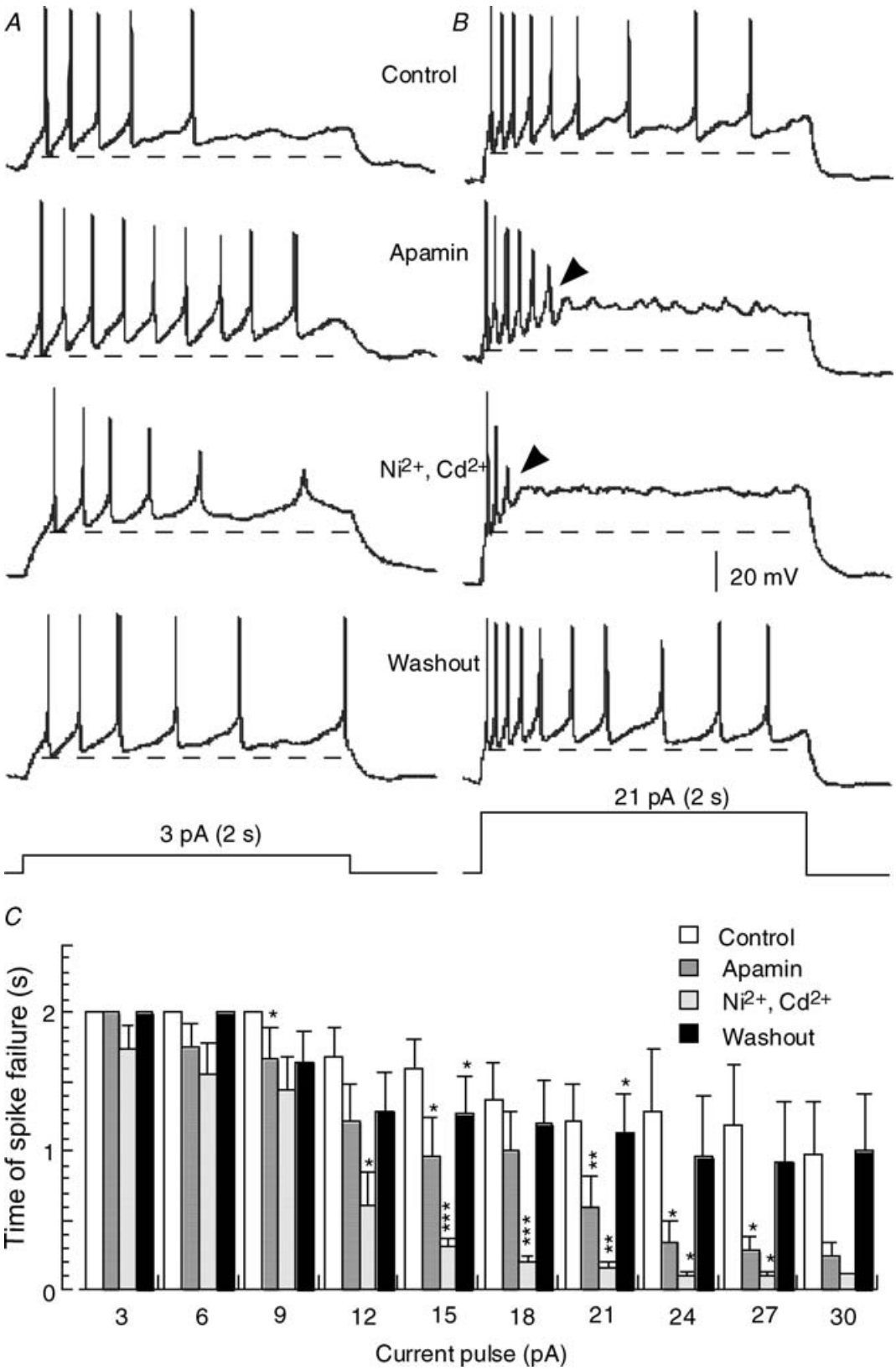

Figure 6. Current pulse-induced spike trains and spike failure
A 2 s current pulse of 3 pA (*A*) or 21 pA (*B*) evoked spike trains are shown. Under control conditions, spike frequency adaptation was seen, especially with a lower amplitude of the current pulse, which was reduced by apamin (*A*). With a higher amplitude of current pulse, apamin caused a rapid reduction in spike amplitude and failure, as

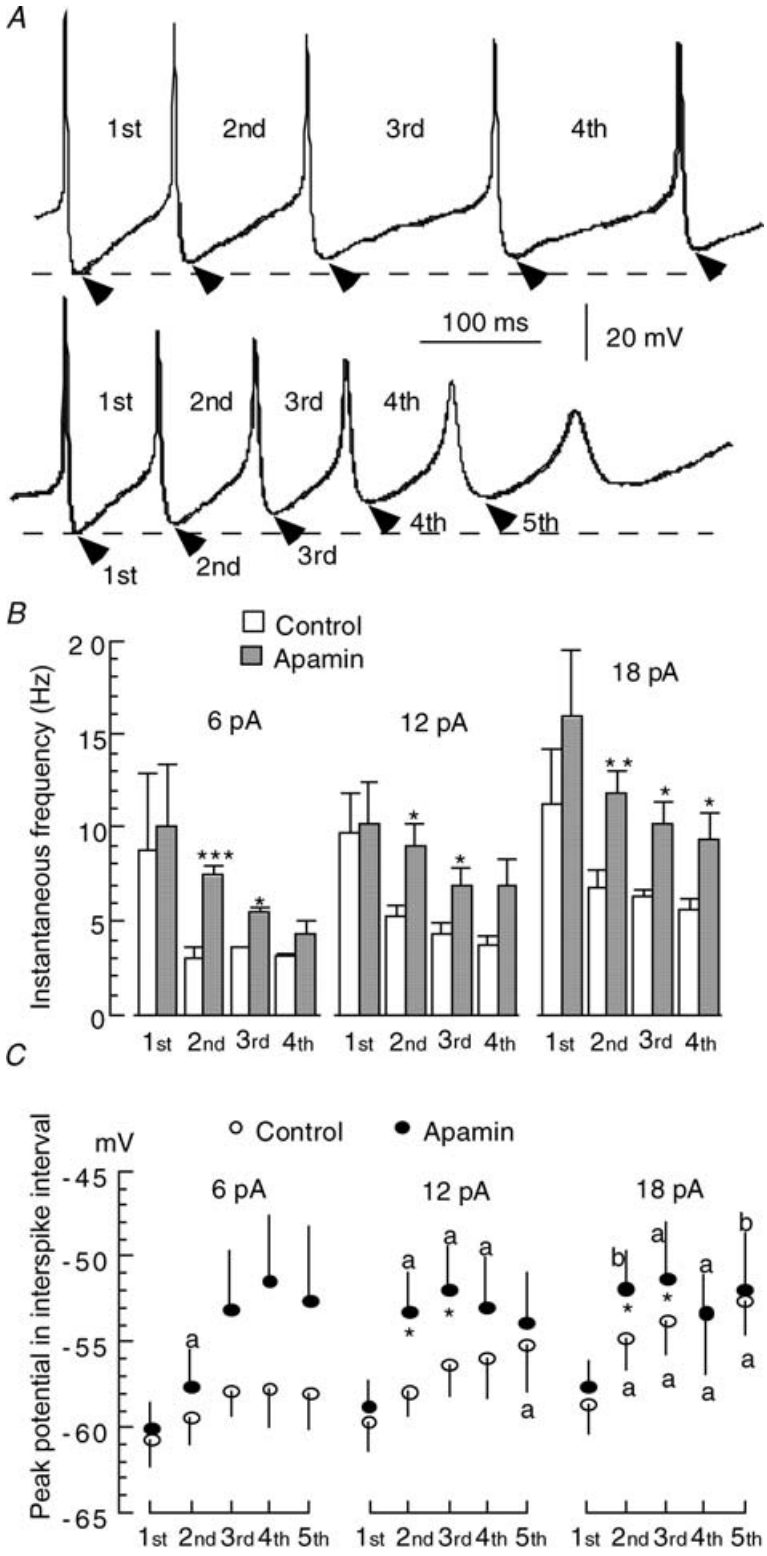

Figure 7. Instantaneous frequency and membrane potential of the interspike interval
A, the initial five spikes evoked by 27 pA current pulse in the control (upper) and in the presence of 100 nM apamin (lower) are shown. Instantaneous spike frequency was calculated by measuring the time of each interspike interval, as indicated by 1st to 4th. The peak potential of the interspike interval is indicated by an arrowhead. The broken line under the voltage trace shows the level of the initial peak potential. *B* and *C*, the instantaneous frequency and peak potential of the interspike interval were plotted against 1st to 4th or 5th, as shown in *A*. The data were obtained with current pulses of 6 pA (left panel), 12 pA (middle) and 18 pA (right). The values in the graphs represent means ± S.E.M. ($n = 3$–11). $^{*}P < 0.05$; $^{**}P < 0.01$; $^{***}P < 0.001$ *versus* control. $^{a}P < 0.05$; $^{b}P < 0.01$ *versus* 1st in either the control or the presence of apamin. The unpaired *t* test (*B*) and paired *t* test (*C*) were used.

indicated by an arrowhead in B. The reduction and failure were more prominent in the presence of Ni^{2+} and Cd^{2+}. When the spike amplitude became less than 10% of the amplitude of the initial spike evoked by the current pulse, it was considered as spike failure. The time of spike failure was defined as the time of the last spike after the onset of the current pulse. *C*, time of spike failure was plotted against the amplitude of the current pulse. The values in the bar graph are means ± S.E.M. ($n = 5$–10). In some cases, S.E.M. was too small to be shown. $^{*}P < 0.05$; $^{**}P < 0.01$; $^{***}P < 0.001$ *versus* control in paired *t* test.

The afterhyperpolarization current, which was blocked by Ni^{2+} and Cd^{2+}, in the adult GnRH neurones, exhibited a decay time constant ranging between 153 ms and 799 ms (Fig. 4*B*), which is classified as I_{sAHP} (for reviews, see Faber & Sah, 2003; Stocker, 2004; Vogalis *et al.* 2003). An afterhyperpolarization current with a shorter decay time constant than 100 ms (medium AHP current) was undetectable in the adult GnRH neurones. Many neurones, including hypothalamic and hippocampal ones, show I_{sAHP} (for a review, see Vogalis *et al.* 2003). The reported I_{sAHP} is insensitive to apamin, whereas I_{mAHP} is blocked by a nanomolar concentration of apamin (Vogalis *et al.* 2003). The channels involved in I_{mAHP} are believed to belong to the SK family, whereas those for I_{sAHP} remain unknown (Vogalis *et al.* 2003). In contrast, the I_{sAHP} observed in the present experiment was blocked by apamin with an IC_{50} of ~100 pM, which is the same concentration as that for the blockade of I_{mAHP} (Vogalis *et al.* 2003). These results lead us to speculate that I_{sAHP} in the rat GnRH neurone could be carried through channels of the SK family, such as SK1, SK2 and SK3, because SK channels are activated by submicromolar concentrations of Ca^{2+} in a voltage-independent manner (Xia *et al.* 1998), and because SK channels are almost completely blocked by apamin (Kohler *et al.* 1996). SK2 and SK3 expressed in *Xenopus* oocytes are potently blocked by apamin with an IC_{50} in the picomolar range (Kohler *et al.* 1996; Ishii *et al.* 1997). SK1 is also blocked by apamin when expressed in a mammalian cell line, but not in *Xenopus* oocytes (Shah & Haylett, 2000; Strobaek *et al.* 2000). In addition, other Ca^{2+}-activated K^+ channels, such as SK4, IK and BK, are not inhibited by apamin (Joiner *et al.* 1997; Ishii *et al.* 1999; Faber & Sah, 2003). In the present study, 20–30% of I_{sAHP} was resistant to apamin (Fig. 3*C*). The channels responsible for this resistant current remain to be determined.

Some reports have suggested that Ca^{2+} influx through certain subtypes of Ca^{2+} channel is related to the generation of a slow AHP (Williams *et al.* 1997; Pineda *et al.* 1998; Wolfart & Roeper, 2002). Therefore, we investigated the effects of subtype-specific Ca^{2+} channel blockers, but found no specificity of Ca^{2+} channel subtypes for the generation of I_{sAHP} in rat GnRH neurones (Fig. 5). All fivesubtypes of Ca^{2+} currents contributed equally to the generation of I_{sAHP} according to the level of contribution to the total Ca^{2+} current. This is reasonable and supports the possible involvement of SK channels, because the K_D of Ca^{2+} for the activation of SK channels is 0.3 μM and full activation is achieved with a submicromolar concentration of Ca^{2+} (Xia *et al.* 1998). For such concentrations of Ca^{2+}, the channels need not to be closely located to the Ca^{2+} channels. In the present experiment, however, we did not examine the specific contribution of each Ca^{2+} channel to the apamin-sensitive component of I_{sAHP}. In addition to the electrophysiological observations, GnRH neurones expressed mRNA for *SK1–3* (Fig. 8). Single-cell RT-PCR analysis revealed the presence of *SK1* mRNA in ~40% of the GnRH neurones examined. Transcripts for SK2 and SK3 were detected in ~80% of the GnRH neurones. These findings are in accord with a previous report that guinea pig GnRH neurones express *SK3* mRNA and exhibit an AHP (Bosch *et al.* 2002). Taken together, it is likely that GnRH neurones possess functional SK channels.

To investigate the physiological role of this apamin-sensitive I_{sAHP}, we carried out a current-clamp experiment (Figs 6 and 7). GnRH neurones showed beating-type firing with a maximum frequency of less than 33 Hz, which suggests that the rat GnRH neurone is a slow-spiking neurone. The mouse GnRH neurone shows a similar firing property (Suter *et al.* 2000; Sim *et al.* 2001; Kuehl-Kovarik *et al.* 2002). The spontaneous action potentials of isolated mouse GnRH neurones consist of brief bursts of 2–20 Hz, separated by 1–10 s. Spike-dependent depolarizing afterpotentials are thought to contribute to these bursting activities (Kuehl-Kovarik *et al.* 2005). We did not examine whether rat GnRH neurones exhibited a brief burst, because we recorded a train of action potentials evoked by 2 s current pulse. Blockade of I_{sAHP} by apamin caused spike failure, especially when a high-intensity current pulse was applied. The membrane potential in the interspike interval became progressively depolarised, and the cells could finally generate no action potentials. The application of Ni^{2+} and Cd^{2+}, which completely blocks both I_{sAHP} and Ca^{2+} currents, further accelerated the spike failure. These findings suggest that I_{sAHP} is activated by action potentials and causes spike frequency adaptation with a moderate depolarizing input, and that this current may support persistent firing with a relatively strong depolarizing input. An LH surge lasts a few hours, during which GnRH neurones are likely to generate action potentials either continuously or intermittently with bursts. Although the mechanism is not known, it is

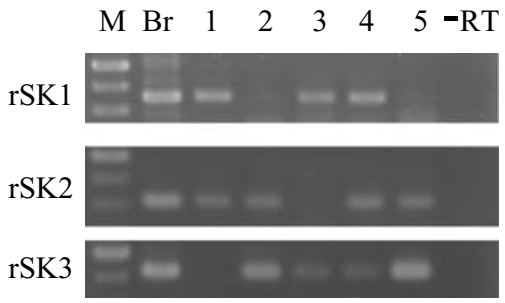

Figure 8. Single-cell RT-PCR analysis of the *SK1–3* mRNA in single GnRH neurones
Each single cell was examined with only one primer (rSK1, rSK2 or rSK3). The gel shows the presence of 361 bp SK1, 314 bp SK2 and 422 bp SK3 amplicons. Br, rat brain RNA was used as a template for positive control. −RT, RNA was treated without reverse transcriptase. M, 100 bp DNA ladder with a thick band of 500 bp.

probable that GnRH neurones receive a relatively strong persistent depolarizing input during an LH surge. In this situation, I_{sAHP} may play an important role in the firing of GnRH neurones.

In conclusion, the rat GnRH neurone expresses voltage-gated Ca^{2+} channels and SK channels, possibly together with unidentified Ca^{2+}-activated voltage-independent K^+ channels. Calcium ions passing through the voltage-gated Ca^{2+} channels activate these Ca^{2+}-activated K^+ channels, which allow the continuous firing of GnRH neurones. Although there was no correlation of the size or decay time constant of I_{sAHP} to the firing pattern of evoked action potentials, this point remains to be analysed in a future experiment on spontaneous and evoked action potentials in slice preparations.

References

Aosaki T & Kasai H (1989). Characterization of two kinds of high-voltage activated Ca-channel currents in chick sensory neurons. *Pflugers Arch* **414**, 150–156.

Blatz AL & Magleby KL (1986). Single apamin-blocked Ca-activated K^+ channels of small conductance in cultured rat skeletal muscle. *Nature* **323**, 718–720.

Boll W & Lux HD (1985). Action of organic antagonists on neuronal calcium currents. *Neurosci Lett* **56**, 335–339.

Bosch MA, Kelly MJ & Ronnekleiv OK (2002). Distribution, neuronal colocalization, and 17β-E2 modulation of small conductance calcium-activated K^+ channel (SK3) mRNA in the guinea pig brain. *Endocrinology* **143**, 1097–1107.

Catterall WA (2000). Structure and regulation of voltage-gated Ca^{2+} channels. *Ann Rev Cell Dev Biol* **16**, 521–555.

Faber ESL & Sah P (2003). Calcium-activated potassium channels: multiple contributions to neuronal function. *Neuroscientist* **9**, 181–194.

Garcia ML, Hanner M, Knaus HG, Koch R, Schmalhofer W, Slaughter RS & Kaczorowski GJ (1997). Pharmacology of potassium channels. *Adv Pharmacol* **39**, 425–471.

Hille B (2001). *Ion Channels of Excitable Membranes*. Sinauer, Sunderland, MA.

Ishii TM, Maylie J & Adelman JP (1997). Determinants of apamin and D-tubocurarine block in SK potassium channels. *J Biol Chem* **272**, 23195–23200.

Ishii TM, Silvia C, Hirschberg B, Bond CT, Adelman JP & Maylie J (1999). A human intermediate conductance calcium-activated potassium channel. *Proc Natl Acad Sci U S A* **94**, 11651–11656.

Jan LY & Jan YN (1997). Cloned potassium channels from eukaryotes and prokaryotes. *Ann Rev Neurosci* **20**, 91–123.

Joiner WJ, Wang L-Y, Tang MD & Kaczmarek LK (1997). hSK4, a member of a novel subfamily of calcium-activated potassium channels. *Proc Natl Acad Sci U S A* **94**, 11013–11018.

Kato M, Watanabe M & Sakuma Y (2003). Characterization of voltage-gated calcium currents in gonadotropin-releasing hormone neurons tagged with green fluorescent protein in rats. *Endocrinology* **144**, 5118–5125.

Kohler M, Hirschberg B, Bond CT, Kinzie JM, Marrion NV, Maylie J & Adelman JP (1996). Small-conductance, calcium-activated potassium channels from mammalian brain. *Science* **273**, 1709–1714.

Kuehl-Kovarik MC, Partin KM, Handa RJ & Dudek FE (2005). Spike-dependent depolarizing afterpotentials contribute to endogenous bursting in gonadotropin releasing hormone neurones. *Neuroscience* **134**, 295–300.

Kuehl-Kovarik MC, Pouliot WA, Halterman GL, Handa RJ & Dudek FE (2002). Episodic bursting activity and response to excitatory amino acids in acutely dissociated gonadotropin-releasing hormone neurons genetically targeted with green fluorescent protein. *J Neurosci* **22**, 2313–2322.

Newcomb R, Szoke B, Palma A, Wang G, Chen X-H, Hopkins W, Cong R, Miller J, Urge L, Tarczy-Hornoch K, Loo JA, Dooley DJ, Nadasdi L, Tsien RW, Lemos J & Miljanich G (1998). Selective peptide antagonist of the class E calcium channel from the venom of the tarantula *Hysterocrates gigas*. *Biochemistry* **37**, 15353–15362.

Nunemaker CS, DeFazio RA & Moenter SM (2003). Calcium current subtypes in GnRH neurons. *Biol Reprod* **69**, 1914–1922.

Pineda JC, Waters RS & Foehring RC (1998). Specificity in the interaction of HVA Ca^{2+} channel types with Ca^{2+}-dependent AHPs and firing behavior in neocortical pyramidal neurons. *J Neurophysiol* **79**, 2522–2534.

Randall A & Tsien RW (1995). Pharmacological dissection of multiple types of Ca^{2+} channel currents in rat granule neurons. *J Neurosci* **15**, 2995–3012.

Romey G, Hugues M, Schmid-Antomarchi H & Lazdunski M (1984). Apamin: a specific toxin to study a class of Ca^{2+}-dependent K^+ channels. *J Physiol* (Paris) **79**, 259–264.

Sah P (1996). Ca^{2+}-activated K^+ currents in neurons: types, physiological roles and modulation. *Trends Neurosci* **19**, 150–154.

Sailer CA, Hu H, Kaufmann WA, Trieb M, Schwarzer C, Storm JF & Knaus HG (2002). Regional differences in distribution and functional expression of small-conductance Ca^{2+}-activated K^+ channels in rat brain. *J Neurosci* **22**, 9698–9707.

Schwindt PC, Spain WJ, Foering RC, Stafstrom CE, Chubb MC & Crill WE (1988). Mutiple potassium conductances and their functions in neurons from cat sensorimotor cortex *in vitro*. *J Neurophysiol* **59**, 424–449.

Shah M & Haylett DG (2000). The pharmacology of hSK1 Ca^{2+}-activated K^+ channels expressed in mammalian cell lines. *Br J Pharmacol* **129**, 627–630.

Sim JA, Skynner MJ & Herbison AE (2001). Heterogeneity in the basic membrane properties of postnatal gonadotropin-releasing hormone neurons in the mouse. *J Neurosci* **21**, 1067–1075.

Stocker M (2004). Ca^{2+}-activated K^+ channels: molecular determinants and function of the SK family. *Nature Rev Neurosci* **5**, 758–770.

Stocker M, Krause M & Pedarzani P (1999). An apamin-sensitive Ca^{2+}-activated K^+ current in hippocampal pyramidal neurons. *Proc Natl Acad Sci U S A* **96**, 4662–4667.

Strobaek D, Jorgensen TD, Christophersen P, Ahring PK & Olesen S-P (2000). Pharmacological characterization of small-conductance Ca^{2+}-activated K^+ channels stably expressed in HEK293 cells. *Br J Pharmacol* **129**, 991–999.

Suter KJ, Wuarin J-P, Smith BN, Dudek FD & Moenter SM (2000). Whole-cell recordings from preoptic/hypothalamic slices reveal burst firing in gonadotropin-releasing hormone neurons identified with green fluorescent protein in transgenic mice. *Endocrinology* **141**, 3731–3736.

Tottene A, Volsen S & Pietrobon D (2000). α_{1E} subunits from the pore of three cerebellar R-type calcium channels with different pharmacological and permeation properties. *J Neurosci* **20**, 171–178.

Tsien RW, Lipscombe D, Madison DV, Bley KR & Fox AP (1988). Multiple types of neuronal calcium channels and their selective modulation. *Trends Neurosci* **11**, 431–438.

Villalobos C, Shakkottai VG, Chandy KG, Michelhaugh SK & Andrade R (2004). SK_{Ca} channels mediate the medium but not slow calcium-activated afterhyperpolarization in cortical neurons. *J Neurosci* **24**, 3537–3542.

Vogalis F, Storm JF & Lancaster B (2003). SK channels and the varieties of slow after-hyperpolarizations in neurons. *Eur J Neurosci* **18**, 3155–3166.

Watanabe M, Sakuma Y & Kato M (2004). High expression of the R-type voltage-gated Ca^{2+} channel and its involvement in Ca^{2+}-dependent gonadotropin-releasing hormone release in GT1–7 cells. *Endocrinology* **145**, 2375–2383.

Williams S, Serafin M, Muhlethaler M & Bernheim L (1997). Distinct contributions of high- and low-voltage activated calcium currents to afterhyperpolarizations in cholinergic nucleus basalis neurons of the guinea pig. *J Neurosci* **17**, 7307–7315.

Wolfart J & Roeper J (2002). Selective coupling of T-type calcium channels to SK potassium channels prevents intrinsic bursting in dopaminergic midbrain neurons. *J Neurosci* **22**, 3404–3413.

Xia X-M, Fakler B, Rivard A, Wayman G, Johnson-Pais T, Keen JE, Ishii T, Hirschberg B, Bond CT, Lutsenko S, Maylie J & Adelman JP (1998). Mechanism of calcium gating in small-conductance calcium-activated potassium channels. *Nature* **395**, 503–507.

Zang L & Krnjevic K (1987). Apamin depresses selectively the after-hyperpolarization of cat spinal motoneurons. *Neurosci Lett* **74**, 58–62.

Acknowledgements

We are grateful to Drs Y. Hiraizumi, I. Nishimura, S. Sato, and S. Yin for their technical assistance, and to Dr T. Hamada for his valuable advice regarding the molecular biology experiment. This work was supported in part by Grants-in-Aid for Scientific Research, 16590180, from the Japan Society for the Promotion of Science and, 16086210, from the Ministry of Education, Culture, Sports, Science and Technology of Japan.

Supplemental material

The online version of this paper can be accessed at:
DOI: 10.1113/jphysiol.2006.110155
http://jp.physoc.org/cgi/content/full/jphysiol.2006.110155/DC1
and contains supplemental material consisting of two figures.

Supplemental Figure 1. Afterhyperpolarization current in an acute slice preparation

Supplemental Figure 2. Spike failure under the control conditions

This material can also be found as part of the full-text HTML version available from http://www.blackwell-synergy.com